Elastic properties of a Poisson–Shear material

TEIK-CHENG LIM
Nanoscience and Nanotechnology Initiative, Faculty of Engineering, The National University of Singapore, 9 Engineering Drive 1, S 117576, Republic of Singapore
E-mail: alan_tc_lim@yahoo.com

A Poisson–Shear material is one which displays significant in-plane shear strain when loaded in the out-of-plane direction. Hence for a prescribed out-of-plane strain (ε_3), we have $\varepsilon_1 \approx -\varepsilon_2$. To attain this behavior a Poisson–Shear material should, for example, possess a positive Poisson's ratio in the 1–3 plane but a negative Poisson's ratio in the 2–3 plane, or vice versa, such that the magnitudes are almost equal. A Poisson–Shear material, therefore, can be used as a micro-capsule for squeezing into veins or any small ducts such that axis-1 is parallel to the micro-duct. Hence when squeezed along axis-3 the micro-capsule contracts along axis-2, or vice versa, such that the transverse cross-section of the micro-capsule contracts to ease entry. Allowance for expansion along axis-1, on the other hand, prevents excessive densification, hence enabling the micro-capsule to perform as drug-delivery media or for any storage purposes during transport (see Fig. 1 for illustration). Based on strain energy formulation, the Poisson's ratio is in the range $-1 < v < 0.5$ [1]. Almost all known materials, however, exhibit positive Poisson's ratio within the range $0 < v < 0.5$. Negative Poisson' ratio material (also known as "auxetic" material) has been investigated by Lakes *et al*. [2–10], Evans *et al*. [11–19], Scarpa *et al*. [20–22], Baughman *et al*. [23, 24], Sigmund [25], and Griffin *et al*. [26]. The auxetic behavior can be attained via re-entrant structures (e.g. [9, 16, 22]), chiral honeycomb structures (e.g. [7]), rotating structures (e.g. [17, 18]) and molecular arrangement (e.g. [13, 26]). Large positive Poisson's ratio [27], on the other hand, can be attained through hexagonal honeycomb structure, as shown in Fig. 2a, which is an anti-thesis of the re-entrant structure, as depicted in Fig. 2b. In recent years it has been shown that a combination of both positive and negative Poisson's ratio leads to unique properties. For example, a beam that is functionally graded from positive Poisson's ratio on the top surface to a negative Poisson's ratio at the bottom surface has been shown to exhibit Poisson-curving behavior, i.e. prescription of curving gives significant thickening or thinning depending on the direction of bending [28]. Alternatively when a material possesses a positive Poisson's ratio in one plane (such as 2–3 plane) and a negative Poisson's ratio in another plane (such as 1–3 plane), then significant 1–2 plane shearing is observed when normal strain is prescribed in the 3-direction [29]. Schematically, a Poisson–Shear material can be obtained via merger of Fig. 2a and b, i.e. hexagonal honeycomb structures in the 1–3 plane and re-entrant structures in the 2–3 plane, as furnished by the representative volume element (RVE) in Fig. 3. The top or bottom half of this Poisson–Shear RVE structure can be obtained by folding a sheet of the geometry shown in Fig. 4. Consider an RVE shown in Fig. 3 or Fig. 4 where $L =$ major length before folding, $l =$ minor length before folding, and $b =$ base, with 1 and 2 corresponding to the in-plane principal axes. To give $v < 0$ in 1–3 plane and $v > 0$ in 2–3 plane, we let $0 < \theta_2 < (\pi/2) < \theta_1 < \pi$. Recently, a unified study on the elastic stiffness of a generalized honeycomb structure, applicable for Poisson's ratio of either signs, has been performed [30], whereby the mode of deformation is confined to be two-dimensional. In this paper, we extend a similar approach [30] for the case of Poisson–Shear material [29], in which deformation is three-dimensional.

For brevity, we employ the notation θ_i for $i = 1, 2$. By virtue of symmetry, one quarter of the RVE is isolated for analysis, as shown in Fig. 5. A kinematics proof for Poisson–Shearing is given in the Appendix. In the following analysis, we consider $i, j = 1, 2 \neq 3$ unless specified otherwise. Since $(\mathrm{OC}) = [b_i - (l_i - b_i)\cos\theta_i]/2$ and $(\mathrm{OA}) = [(l_i - b_i)\sin\theta_i]/2$, we have the in-plane extensions

$$u_i = d(\mathrm{OC}) = \left(\frac{l_i - b_i}{2}\right)\sin\theta_i\, d\theta_i \tag{1}$$

and the out-of-plane extension

$$u_3 = d(\mathrm{OA}) = \left(\frac{l_i - b_i}{2}\right)\cos\theta_i\, d\theta_i. \tag{2}$$

Equation 1 shows elongation along axis-1 in terms of rotation of θ_1 hinges and elongation along axis-2 in terms of rotation of θ_2 hinges. Elongation in axis-3 can be described by rotation of θ_1 or θ_2, as shown in Equation 2. From Equation 1, elongation along axis-1 in terms of θ_2 rotation, and vice versa, can be easily obtained:

$$u_i = \left(\frac{l_j - b_j}{2}\right)\tan\theta_i\cos\theta_j\, d\theta_j. \tag{3}$$

The torque, T, required to rotate by an angle $\delta\theta$ is assumed linear for infinitesimal deformation

$$T = k_\theta \delta\theta \tag{4}$$

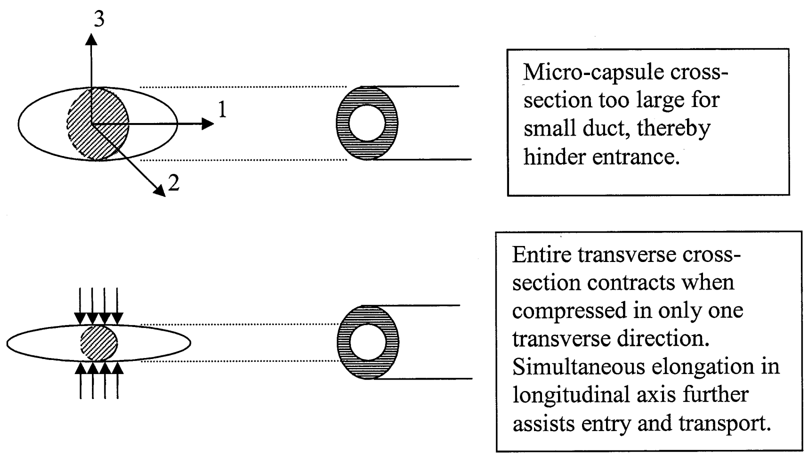

Figure 1 One application of Poisson–Shear material, in which $\upsilon_{31} > 0$ and $\upsilon_{32} < 0$.

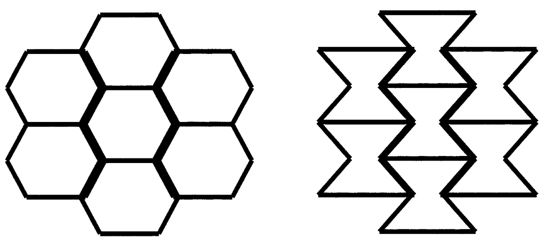

Figure 2 Open structures which give: (a) large positive Poisson's ratio (hexagonal honeycomb) and (b) large negative Poisson's ratio (re-entrant structure).

where k_θ is the rotational stiffness of a hinge. Therefore the potential energy per hinge is

$$U_{\text{hinge}} = \frac{1}{2} k_\theta (\delta\theta)^2. \tag{5}$$

Suppose there are n_1 hinges per RVE rotating in plane 1–3 and n_2 hinges per RVE rotating in plane 2–3, the energy per RVE is

$$U = \frac{n_1}{2} k_{\theta 1} (\delta\theta_1)^2 + \frac{n_2}{2} k_{\theta 2} (\delta\theta_2)^2. \tag{6}$$

The elastic coefficient, C_{ij}, can therefore be obtained via energy approach as [31]

$$C_{ij} = \frac{1}{V_0} \frac{\partial^2 U}{\partial \varepsilon_i \partial \varepsilon_j} \tag{7}$$

where V_0 = volume of the RVE before deformation. For infinitesimal deformation, the change in volume is marginal compared to the initial volume, therefore convenient usage of initial RVE volume is valid. By definition of strain, we have, according to the RVE geometry:

$$\varepsilon_i = \frac{2u_i}{L_i - (l_i - b_i)(1 + \cos\theta_i)} \tag{8}$$

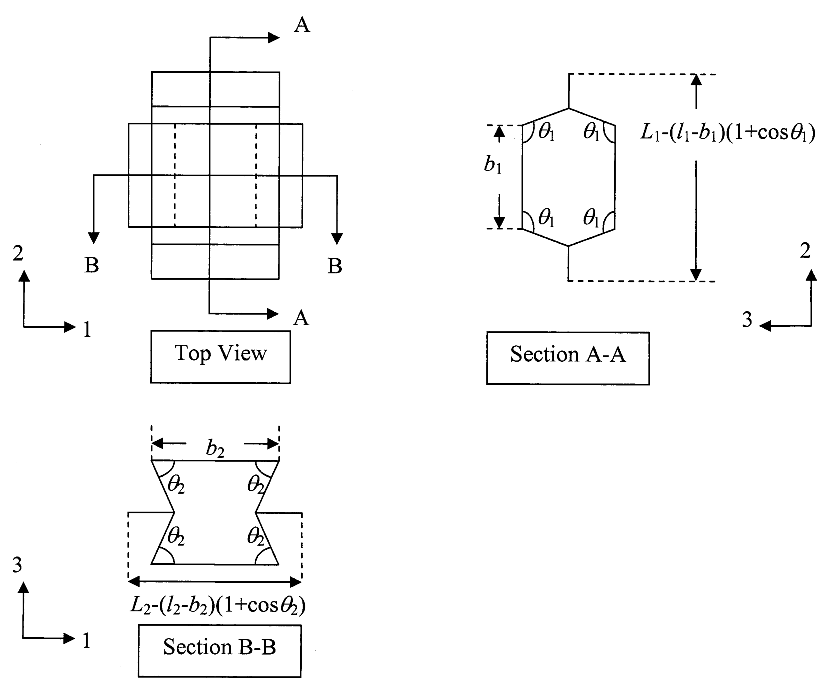

Figure 3 Geometry of combined hexagonal honeycomb and re-entrant structures.

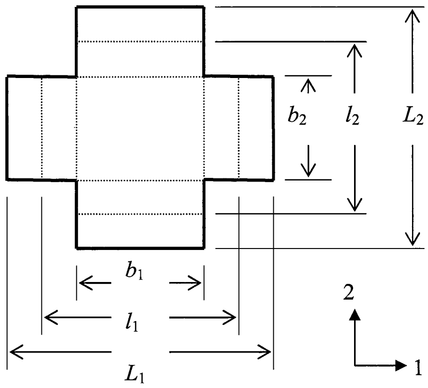

Figure 4 Sheet geometry before folding into top or bottom half of the RVE.

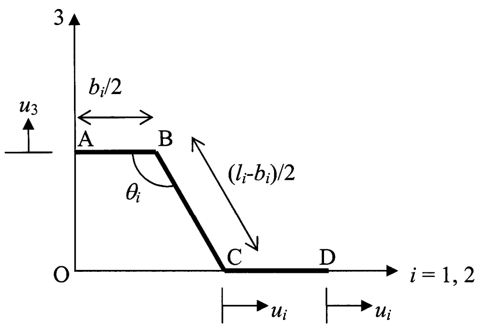

Figure 5 One-quarter of RVE for analysis.

and

$$\varepsilon_3 = \frac{2u_3}{(l_i - b_i)\sin\theta_i}. \tag{9}$$

Substituting Equation 1 into Equation 8 gives

$$d\theta_i = \frac{L_i - (l_i - b_i)(1 + \cos\theta_i)}{(l_i - b_i)\sin\theta_i}\varepsilon_i \tag{10}$$

and Equation 2 into Equation 9 leads to

$$d\theta_i^{**} = \varepsilon_3 \tan\theta_i. \tag{11}$$

To obtain diagonal terms, C_{ii}, we simply take double differential

$$C_{ii} = \frac{1}{V_0}\frac{\partial^2 U}{\partial \varepsilon_i^2}; \quad i = 1,\ 2,\ 3 \tag{12}$$

where the stored energy is expressed in terms of ε_i. From Equation 6,

$$U = \frac{n_i}{2}k_{\theta i}(\delta\theta_i)^2 + \frac{n_j}{2}k_{\theta j}(\delta\theta_j^*)^2 \tag{13}$$

where $\delta\theta_j^*$ is the indirect contribution to ε_i. From Equations 3 and 8,

$$\delta\theta_j^* = \frac{L_i - (l_i - b_i)(1 + \cos\theta_i)}{(l_j - b_j)\tan\theta_i \cos\theta_j}\varepsilon_i. \tag{14}$$

Substituting Equations 10 and 14 into Equation 13 and taking double differential as described by Equation 12, we have

$$C_{ii} = \frac{[L_i - (l_i - b_i)(1 + \cos\theta_i)]^2}{V_0}\left[\frac{n_i k_{\theta i}}{(l_i - b_i)^2 \sin^2\theta_i} + \frac{n_j k_{\theta j}}{(l_j - b_j)^2 \tan^2\theta_i \cos^2\theta_j}\right]. \tag{15}$$

In order to describe $\delta\theta_1$ or $\delta\theta_2$ in terms of ε_3, Equation 11 is substituted into Equation 6 so that Equation 12 becomes

$$C_{33} = \frac{1}{V_0}[n_1 k_{\theta 1}\tan^2\theta_1 + n_2 k_{\theta 2}\tan^2\theta_2]. \tag{16}$$

To obtain C_{12}, we rewrite Equation 6 as

$$U = \frac{n_1}{2}k_{\theta 1}(\delta\theta_1)(\delta\theta_1^*) + \frac{n_2}{2}k_{\theta 2}(\delta\theta_2)(\delta\theta_2^*) \tag{17}$$

where $\delta\theta_1^*$ is expressed in terms of ε_2, and $\delta\theta_2^*$ in terms of ε_1. Substituting Equations 10 and 14 into Equation 17, and taking differential as in Equation 7, we arrive at

$$C_{12} = \frac{\prod_{i=1}^{2}[L_i - (l_i - b_i)(1 + \cos\theta_i)]}{2V_0} \times\left[\frac{n_1 k_{\theta 1}}{(l_1 - b_1)^2 \sin\theta_1 \cos\theta_1 \tan\theta_2} + \frac{n_2 k_{\theta 2}}{(l_2 - b_2)^2 \sin\theta_2 \cos\theta_2 \tan\theta_1}\right]. \tag{18}$$

To obtain C_{13} and C_{23}, Equation 6 is written as

$$U = \frac{n_i}{2}k_{\theta i}(\delta\theta_i)(\delta\theta_i^{**}) + \frac{n_j}{2}k_{\theta j}(\delta\theta_j^*)(\delta\theta_j^{**}) \tag{19}$$

where, as before, $\delta\theta_i$ and $\delta\theta_j^*$ are described by Equations 10 and 14 respectively, in order to be expressed in terms of ε_i. Both $\delta\theta_i^{**}$ and $\delta\theta_j^{**}$ adopt the form shown in Equation 11 in order to be expressible in terms of ε_3. Therefore,

$$C_{i3} = \frac{L_i - (l_i - b_i)(1 + \cos\theta_i)}{2V_0}\left[\frac{n_i k_{\theta i}}{(l_i - b_i)\cos\theta_i} + \frac{n_j k_{\theta j}}{(l_j - b_j)\cos\theta_j}\left(\frac{\tan\theta_j}{\tan\theta_i}\right)\right]. \tag{20}$$

Consider now a special case whereby

(a) the hinge rotational stiffnesses and equal, i.e. $k_{\theta 1} = k_{\theta 2} = k_\theta$;
(b) for a prescribed out-of-plane deformation, we have equal but opposite principal extensions, i.e. $u_1 = -u_2$; and
(c) in-plane dimensions for RVE are equal, i.e. $L_1 - (l_1 - b_1)(1 + \cos\theta_1) = L_2 - (l_2 - b_2)(1 + \cos\theta_2) = W$.

Conditions (b) and (c) imply $(\varepsilon_1/\varepsilon_2) = -1$, i.e. pure in-plane shearing as a result of out-of-plane loading—

hence pure Poisson–Shearing. Since the presently considered RVE geometry has equal number of hinges rotating about their axes parallel to axes 1 and 2, we have $n_1 = n_2 = n$. Suppose, also, that the rotating arms are equal in length such that $(l_1 - b_1) = (l_2 - b_2) = a$, then from Equation 1 we have

$$\text{(i) } \sin\theta_1 = \sin\theta_2 \qquad \text{if} \quad d\theta_1 = d\theta_2$$

or

$$\text{(ii) } \sin\theta_1 = \sin(\pi - \theta_2) \quad \text{if} \quad d\theta_1 = -d\theta_2.$$

Condition (i) applies for large positive Poisson's ratio if $(\pi/2) < \theta_1 = \theta_2 < \pi$ or for negative Poisson's ratio if $0 < \theta_1 = \theta_2 < (\pi/2)$. Condition (ii) applies for Poisson–Shearing, whereby $\theta_1 = \pi - \theta_2$ and $\theta_2 \in [0, (\pi/2)]$. As such, the elastic coefficients C_{ij} for $i, j = 1, 2, 3$ can be simplified to

$$C_{11} = C_{22} = \frac{2K}{\sin^2\theta_2}\left(\frac{W}{a}\right)^2 \tag{21}$$

$$C_{33} = 2K\tan^2\theta_2 \tag{22}$$

$$C_{12} = -\frac{K}{\sin^2\theta_2}\left(\frac{W}{a}\right)^2 \tag{23}$$

$$C_{13} = C_{23} = -\frac{K}{\cos\theta_2}\left(\frac{W}{a}\right) \tag{24}$$

where

$$K = \frac{nk_\theta}{V_0} = 8\frac{k_\theta}{V_0} \tag{25}$$

since there are 8 hinges per RVE in both the 1–3 plane and 2–3 plane, and

$$V_0 = W^2 a\sin\theta_2. \tag{26}$$

In conclusion the Poisson–Shear material has been defined in this paper and, based on a combined hexagonal honeycomb and re-entrant microstructures, its elastic properties are derived for infinitesimal deformation. The elastic coefficients have been arrived at by taking the double derivative of the potential energy of the hinge rotational stiffness with respect to the orthogonal strains. Whilst the diagonal terms (C_{ii} for $i = 1, 2, 3$) are positive as expected, the Poisson–Shear materials, possessing negative Poisson's ratio in one plane, appear to give negative stiffness in the non-diagonal terms (C_{ij} for $i \neq j$). It now remains to be ascertained if any analogy for this negative stiffness can be made with those studied by Lakes *et al.* [32–34].

Appendix

From the definition of Poisson's ratio and using Equations 8 and 9,

$$v_{3i} = -\frac{\varepsilon_i}{\varepsilon_3} = -\frac{u_i}{u_3}\left[\frac{(l_i - b_i)\sin\theta_i}{L_i - (l_i - b_i)(1 + \cos\theta_i)}\right] \tag{A1}$$

Substituting Equations 1 and 2 into Equation A1,

$$v_{3i} = -\frac{(l_i - b_i)\sin\theta_i\tan\theta_i}{L_i - (l_i - b_i)(1 + \cos\theta_i)}. \tag{A2}$$

Since both $(l_i - b_i)$ and $[L_i - (l_i - b_i)(1 + \cos\theta_i)]$ will have to be positive in order to be physically realizable, the sign for Equation (A2) is determined by θ_i. For $(\pi/2) < \theta_1 < \pi$, we have $\sin\theta_1 > 0$ but $\tan\theta_1 < 0$. Therefore $v_{31} > 0$. For $0 < \theta_2 < (\pi/2)$, we have $\sin\theta_2 > 0$ and $\tan\theta_2 > 0$. Hence $v_{32} < 0$. Defining the Poisson–Shear ratio of maximum in-plane shear strain to the out-of-plane normal strain, we have

$$v_{\text{shear}} = \frac{\gamma_{12}}{\varepsilon_3} = \frac{\varepsilon_1 - \varepsilon_2}{\varepsilon_3} = -v_{31} + v_{32}. \tag{A3}$$

For the special case where $L_1 - (l_1 - b_1)(1 + \cos\theta_1) = L_2 - (l_2 - b_2)(1 + \cos\theta_2)$, $(l_1 - b_1) = (l_2 - b_2)$ and $\theta_1 = \pi - \theta_2$, then upon substitution from Equations A2, A3 becomes

$$v_{\text{shear}} = -2v_{31} = 2v_{32}. \tag{A4}$$

For example, if $b_1 = b_2 = 1.5$ units, $l_1 = l_2 = 3.5$ units, $L_1 = 3.5$ units, $L_2 = 5.5$ units, $\theta_1 = (2\pi/3)$ radian, and $\theta_2 = (\pi/3)$ radian, then $v_{32} = -v_{31} = 1.2$ and hence $v_{\text{shear}} = 2.4$.

References

1. Y. C. FUNG, "Foundations of Solid Mechanics" (Prentice-Hall, New Jersey, 1968).
2. R. S. LAKES, *Science* **235** (1987) 1038.
3. *Idem.*, *ibid.* **238** (1987) 551.
4. *Idem.*, *J. Appl. Mech.* **59** (1992) 744.
5. J. B. CHOI and R. S. LAKES, *Int. J. Mech. Sci.* **37** (1995) 51.
6. C. P. CHEN and R. S. LAKES, *J. Eng. Mater. Technol.* **118** (1996) 285.
7. D. PRALL and R. S. LAKES, *Int. J. Mech. Sci.* **39** (1997) 305.
8. J. B. CHOI and R. S. LAKES, *Int. J. Fracture* **80** (1996) 73.
9. R. S. LAKES, *Science* **288** (2000) 1976.
10. R. S. LAKES and R. WITT, *Int. J. Mech. Eng. Educ.* **30** (2002) 50.
11. B. D. CADDOCK and K. E. EVANS, *J. Phys. D Appl. Phys.* **22** (1989) 1877.
12. K. E. EVANS and B. D. CADDOCK, *ibid.* **22** (1989) 1883.
13. M. A. NKANSAH, K. E. EVANS and I. J. HUTCHINSON, *Model. Simul. Mater. Sci.* **2** (1994) 337.
14. A. ALDERSON and K. E. EVANS, *J. Mater. Sci.* **32** (1997) 2797.
15. K. L. ALDERSON, A. ALDERSON and K. E. EVANS, *J. Strain Anal. Eng. Des.* **32** (1997) 201.
16. K. E. EVANS and A. ALDERSON, *Adv. Mater.* **12** (2000) 617.
17. J. N. GRIMA and K. E. EVANS, *J. Mater. Sci. Lett.* **19** (2000) 1563.
18. C. W. SMITH, J. N. GRIMA and K. E. EVANS, *Acta Mater.* **48** (2000) 4349.
19. A. ALDERSON and K. E. EVANS, *Phys. Chem. Miner.* **28** (2001) 711.
20. F. SCARPA and G. TOMLINSON, *J. Sound Vib.* **230** (2000) 45.
21. F. SCARPA and P. J. TOMLIN, *Fatigue Fracture Eng. Mater.* **23** (2000) 717.
22. F. SCARPA, P. PANAYIOTOU and G. TOMLINSON, *J. Strain Anal. Eng. Des.* **35** (2000) 383.
23. R. H. BAUGHMAN, J. M. SHACKLETT, A. A. ZAKHIDOV and S. STAFSTROM, *Nature* **392** (1998) 362.

24. R. H. BAUGHMAN, S. O. DANTAS, S. STAFSTROM, A. A. ZAKHIDOV, T. B. MITCHELL and D. H. E. DUBIN, *Science* **288** (2000) 2018.
25. O. SIGMUND, *J. Mech. Phys. Solids* **48** (2000) 397.
26. A. C. GRIFFIN, *Macromolecules* **31** (1998) 3145.
27. T. LEE and R. S. LAKES, *J. Mater. Sci*. **32** (1997) 2397.
28. T. C. LIM, *J. Mater. Sci. Lett*. **21** (2002) 1899.
29. *Idem., ibid.* **21** (2002) 1595.
30. *Idem., ibid.* **22** (2003) 1783.
31. J. F. NYE, "Physical Properties of Crystals" (Oxford University Press, Oxford, 1985).
32. R. S. LAKES, *Phil. Mag. Lett*. **81** (2001) 95.
33. *Idem., Nature* **410** (2001) 565.
34. *Idem., J. Mech. Phys. Solids* **50** (2002) 979.

Received 22 December 2003
and accepted 6 April 2004